

## Supplementary Information

# Mechanism of galvanic reduction of selenate oxyanions and surface immobilization by nano zero-valent iron aggregates under anaerobic condition: towards high electron efficiency

Konstantina Chalastara<sup>1</sup> and George P. Demopoulos<sup>1\*</sup>

<sup>1</sup> Materials Engineering, McGill University, Montreal, QC, Canada, H3A0C5

\* Correspondence: [george.demopoulos@mcgill.ca](mailto:george.demopoulos@mcgill.ca); <https://orcid.org/0000-0001-8112-5339>

## 1. Thermodynamic diagrams

Selenium and iron speciation distribution plots are shown in Figure S 1(a) and the speciation diagram of Se(VI) and Se(IV) are presented in Figure S 1(b) obtained by OLI Systems software.

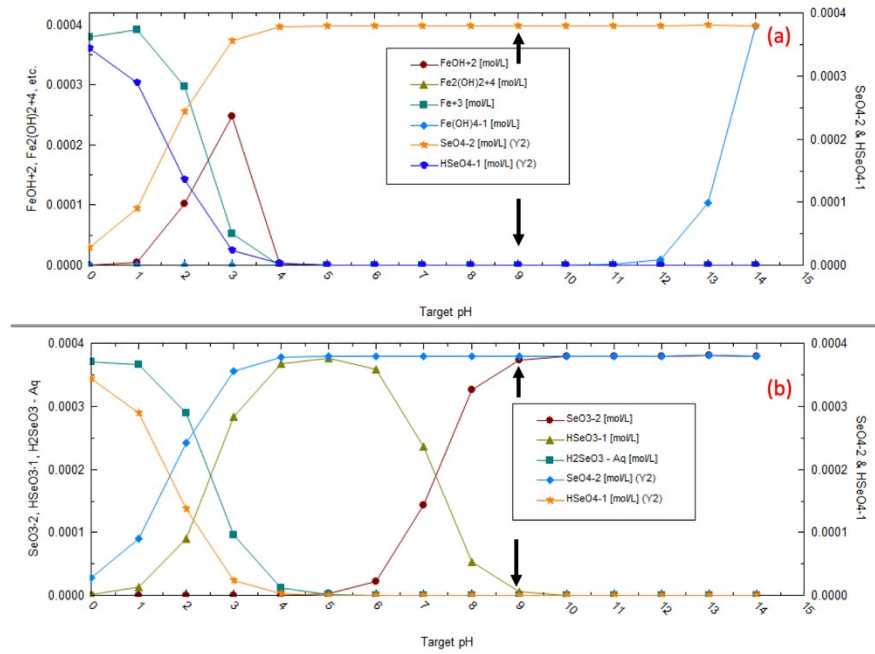


Figure S 1 Speciation diagrams of (a) Se(VI) and Fe(III); and (b) Se(IV) vs. Se(VI). [Se]= 0.38 mM and Fe=0.75 mM.

The Pourbaix diagram for the Se-Fe-H<sub>2</sub>O system shown below in Figure S 1 was built at 25 °C and activity of Se ( $0.38 \cdot 10^{-3}$  M) and Fe ( $0.75 \cdot 10^{-3}$  M) species using the FactSage software

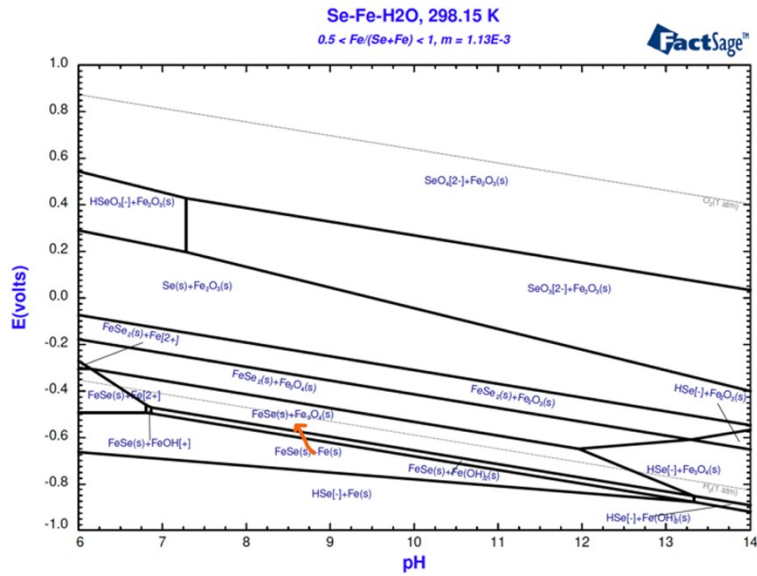


Figure S 2 Pourbaix diagram of Fe (0.75 mM) and Se (0.38 mM) at room temperature prepared using FactSage.

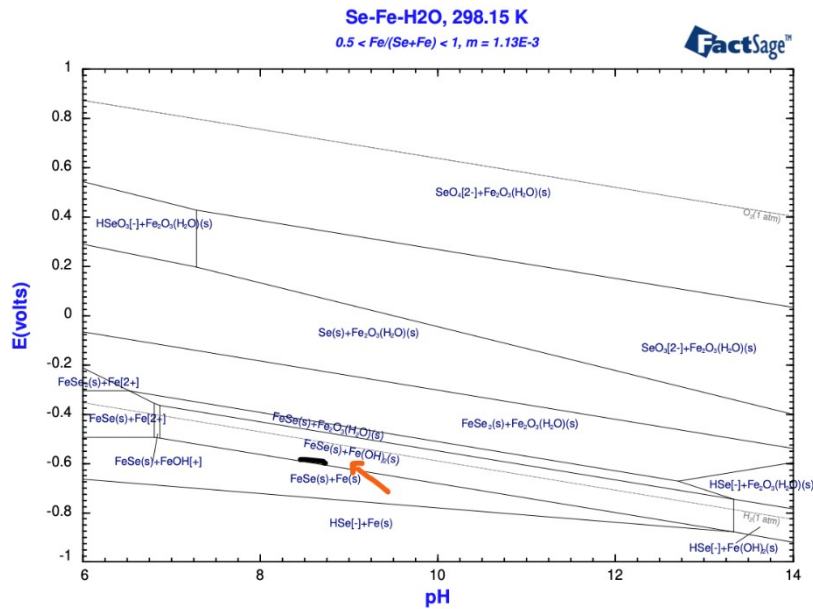
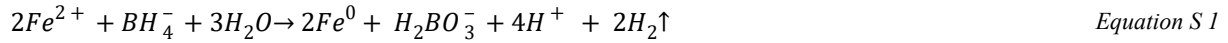


Figure S 3 Pourbaix diagram of Fe (0.75 mM) and Se (0.38 mM) at room temperature prepared with FactSage excluding crystalline iron oxides so metastable hydrous iron oxides become visible.

## 2. nZVI synthesis reaction with $Fe^{2+}$

The nano zero valent iron synthesis took place in a anaerobic chamber using a method similar to previous studies [1], by reacting 100 mL of nitrogen-purged 0.3 M  $FeSO_4 \cdot 7H_2O$  (in 30% ethanol) with 15 mL of 1.3 M  $NaBH_4$  added drop-wise at a 5 mL/min rate. The relevant reaction is given below:



## 3. pH range after nZVI synthesis and Se removal

The pH values of the nZVI synthesis, before the addition of  $NaBH_4$  (pre synthesis pH), after the nZVI synthesis (post synthesis pH) and after the selenium removal pH are shown in Table S 1 for different synthesis experiments for reproducibility purposes.

Table S 1 pH values, before nZVI synthesis, post nZVI synthesis and after selenate removal.

	pre synthesis pH	post synthesis pH	pH <sub>-post Se deposition</sub>
exp-1			9.71
exp-2	4.2	9.18	9.4
exp-3			9.61
exp-4	4.1	9.21	n/a
exp-5			9.79
exp-6	4.3	9.12	n/a
exp-7			10.2
exp-8	4.01	9.22	n/a
exp-9			n/a
exp-10	4.2	9.1	9.92
exp-11			9.45
Average	4.15 ±0.12	9.18 ±0.04	9.72 ±0.27

#### 4. Reproducibility and actual concentration data

The selenium removal data during the reduction tests for various nZVI loadings; 0.15, 1, 1.5, and 3 g/L are presented in Table S 2. Data correspond to Figure 3(a).

Table S 2 Selenium removal data, nZVI loading effect. Data corresponding to Figure 3(a).

Time (min)	nZVI load (g/L)		0.15		1		1.5		3	
	$C_{Se(aq)}$ (mg/L)	STD	$C_{Se(aq)}$ (mg/L)	STD	$C_{Se(aq)}$ (mg/L)	STD	$C_{Se(aq)}$ (mg/L)	STD	$C_{Se(aq)}$ (mg/L)	STD
0	32.50	0.01	32.54	0.01	32.19	0.00	29.54	0.00		
15	25.23	0.01	17.00	0.01	8.14	0.04	3.00	0.07		
30	20.00	0.04	11.00	0.04	3.27	0.02	2.00	0.04		
60	12.94	0.03	5.43	0.03	1.67	0.03	1.00	0.03		
90	10.00	0.03	3.00	0.02	1.20	0.01	0.30	0.02		
150	1.64	0.03	1.64	0.02	0.50	0.00	0.01	0.01		
210	0.02	0.00	N/D*	-	N/D*	-	N/D*	-		

\* not detected – below detection limit (=0.005mg/L)

The selenium removal data during the reduction experiments with various Se starting concentrations,  $C_{Se}$  at 1, 5, 10, and 30 mg/L, are presented in Table S 3, where 1 g/L nZVI loading was used.

Table S 3 Selenium removal data at 1 g nZVI/L loading, Se(VI) concentration effect.

Time (min)	$C_{0(Se)}$ (mg/L)			
	1	5	10	30

	<b>C<sub>Se(aq)</sub></b>	<b>STD</b>	<b>C<sub>Se(aq)</sub></b>	<b>STD</b>	<b>C<sub>Se(aq)</sub></b>	<b>STD</b>	<b>C<sub>Se(aq)</sub></b>	<b>STD</b>
0	1.02	0.00	5.4	0.01	9.23	0.01	32.54	0.01
15	0.04	0.01	1.04	0.01	0.29	0.02	17.00	0.01
30	N/D*	-	0.03	0.01	0.15	0.01	11.00	0.04
60	N/D*	-	N/D*	-	0.07	0.03	5.43	0.03
90	N/D*	-	N/D*	-	0.05	0.0	3.00	0.02
150	N/D*	-	N/D*	-	N/D*	-	1.64	0.02
210	N/D*	-	N/D*	-	N/D*	-	N/D*	-

\* not detected – below detection limit (=0.005 mg/L)

## 5. Kinetics

First-order kinetic plots of the selenium batch reaction with nZVI are shown in Figure 3(b). Based on Equation S 2 and the apparent rate constant  $k_{ap}$ , the specific rate constants (per unit mass,  $k_m$  or surface area,  $k_A$  of nZVI) are extracted and presented in Table S 4:

$$\ln(C/C_0) = -k_{ap} * t \quad \text{Equation S 2}$$

Where:  $k_{ap} = k * m_{Fe}$  or  $k * A_{surf}$

$$k_{ap} = 20 * 10^{-3} \text{ min}^{-1} \text{ (from Figure 3(b))}$$

Table S 4 Specific rate constants (per unit mass or surface area of nZVI) extracted from first order kinetic plots of Figure 3(b).

<b>m<sub>Fe</sub> (g/L)</b>	<b>k<sub>m</sub> (x 10<sup>-3</sup> g<sup>-1</sup> * min<sup>-1</sup>)</b>	<b>k<sub>A</sub> (x 10<sup>-3</sup> m<sup>-2</sup> * min<sup>-1</sup>)</b>
0.15	133	7.84
1	20	1.17
1.5	13.3	0.78
3	6	0.39

## 6. Gas chromatography for H<sub>2</sub> Determination

Gas chromatography measurements were made by using a sealed vial with a known volume that the gas can disperse in, and by adding specific quantity of synthesized nZVI in HCl solution, the quantity of Fe<sup>0</sup> determined with the aid of Equation S 3:



More specifically, the Fe<sup>0</sup> content of the nZVI<sub>bare</sub> and nZVI<sub>post</sub> was determined by dissolving 30 mg into 60 mg degassed 12 N HCl and measuring the H<sub>2</sub> produced, as per procedure provided by Li et al. [2].

The hydrogen calibration curve seen in Figure S 4, coefficient of determination R<sup>2</sup>=0.998, correlates the peak areas to different known concentrations of the gas. Calibration standards were prepared by adding known quantities of the gas in the vial without nZVI.

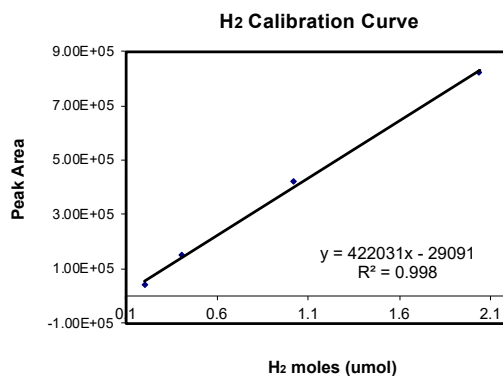


Figure S 4 Hydrogen calibration curve for Fe<sup>0</sup> determination by gas chromatography.

## 7. Electron Efficiency Calculation (E%)

For the estimation of EE(%) the equation proposed by Hong Liu et al. [3] was used after some simplifying modification. The relevant equation is shown below, where  $N_{e,Se}$  is the number of electrons utilized for the reduction of Se(VI) (6 e<sup>-</sup>/mol as per reduction half-reaction:  $\text{Se}^{6+} + 6\text{e}^- \rightarrow \text{Se}^0$ ) and  $N_{e,Fe,total \text{ or } reacted}$  is either the total number of electrons that can be supplied by nZVI (if

all of it reacts) ( $N_{e,Fe,total}$ ) or more strictly is the number of electrons released by the amount of iron oxidized ( $Fe^0 \rightarrow Fe^{2+} + 2e^-$ ) only ( $N_{e,Fe,reacted}$ ). The definition of EE(%) on the basis of  $N_{e,Fe,reacted}$  – that was proposed by Hong Liu et al. – we call it true EE ( $EE_{true}$ ).

$$EE(\%) = \left( \frac{N_{e,Se}}{N_{e,Fe,total \text{ or reacted}}} \right) * 100 \quad \text{Equation S 4}$$

Example 1. Calculation of EE(%) for the case of 0.15 g/L nZVI test:

$$N_{e,Se} = 30 \text{ mg/L Se(VI)} \div 79 \text{ mg/mmol} \times 6 \text{ e}^-/\text{mmol} = 2.28$$

$$N_{e,Fe,total} = 150 \text{ mg/L Fe} \div 56 \text{ mg/mmol} \times 2 \text{ e}^-/\text{mmol} = 5.34$$

$$EE(\%) = \left( \frac{N_{e,Se}}{N_{e,Fe,total}} \right) * 100 = 42.7\%$$

Example 2. Calculation of EE(%) for the case of 1.5 g/L nZVI test

$$N_{e,Se} = 30 \text{ mg/L Se(VI)} \div 79 \text{ mg/mmol} \times 6 \text{ e}^-/\text{mmol} = 2.28$$

$$N_{e,Fe,total} = 1500 \text{ mg/L Fe} \div 56 \text{ mg/mmol} \times 2 \text{ e}^-/\text{mmol} = 53.4$$

$$EE(\%) = \left( \frac{N_{e,Se}}{N_{e,Fe,total}} \right) * 100 = 4.2\%$$

Re-calculating EE(%) now using  $N_{e,Fe,reacted}$ , i.e. the **true EE** we obtain:

Note that based on the analysis reported on Table 1 only 12% of nZVI reacted, i.e.

$$N_{e,Fe,reacted} = 0.12 \times N_{e,Fe,total} = 0.12 \times 53.4 = 6.4$$

$$N_{e,Se} = 30 \text{ mg/L Se(VI)} \div 79 \text{ mg/mmol} \times 6 \text{ e}^-/\text{mmol} = 2.28$$

$$True\_EE(\%) = \left( \frac{N_{e,Se}}{N_{e,Fe,reacted}} \right) * 100 = 35.6\%$$

Or if we only consider the electrons supplied by nZVI during Se deposition (corresponding to 6% nZVI consumption-see Table 1) the true EE becomes 71.2 %.

## 8. BET Analysis

Figure S 5 shows the Brunauer-Emmett-Teller (BET) isotherms for the nZVI NPs before and after reaction with Se(VI). The pore size distribution was determined using the Barret-Joyner-Halender (BJH) method via the adsorption branch of the isotherm, see Figure S 5(insets) [4].

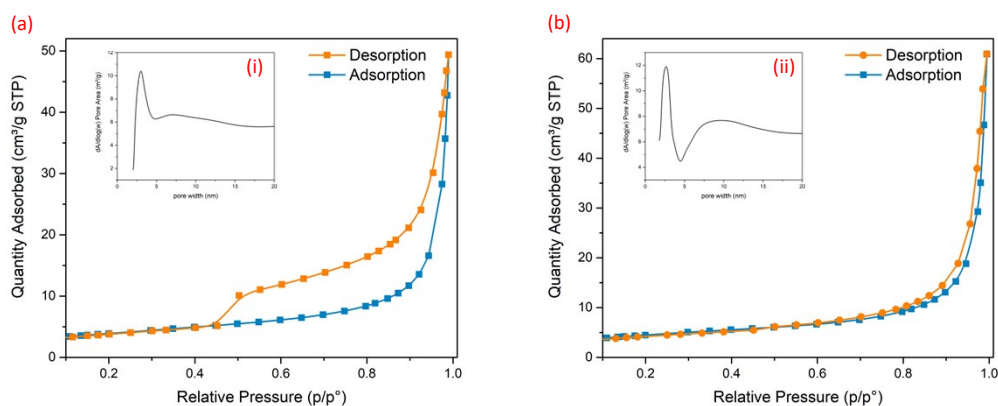


Figure S 5  $N_2$  adsorption–desorption BET isotherms of synthesized and post-reaction nZVI nanoparticles (a) bare and (b) post selenate removal; insets (i,ii) show the BJH pore size distributions.

## 9. STEM-EDS Mapping

To further characterize the elemental distributions on the nZVI<sub>post</sub> particle aggregates following reaction with Se(VI), TEM EDS mapping was performed. In Figure S 6, an HAADF image (a) along STEM-EDS elemental maps for Fe, O, Se individually (b,c,d) and all three elements together (e) clearly show Se to have uniformly deposited across the whole aggregate. The EDS elemental

line profile, with an orange line A to B seen in Figure S 6(e), can be observed in Figure S 6(f) where the relative intensity of each element is monitored across the line.

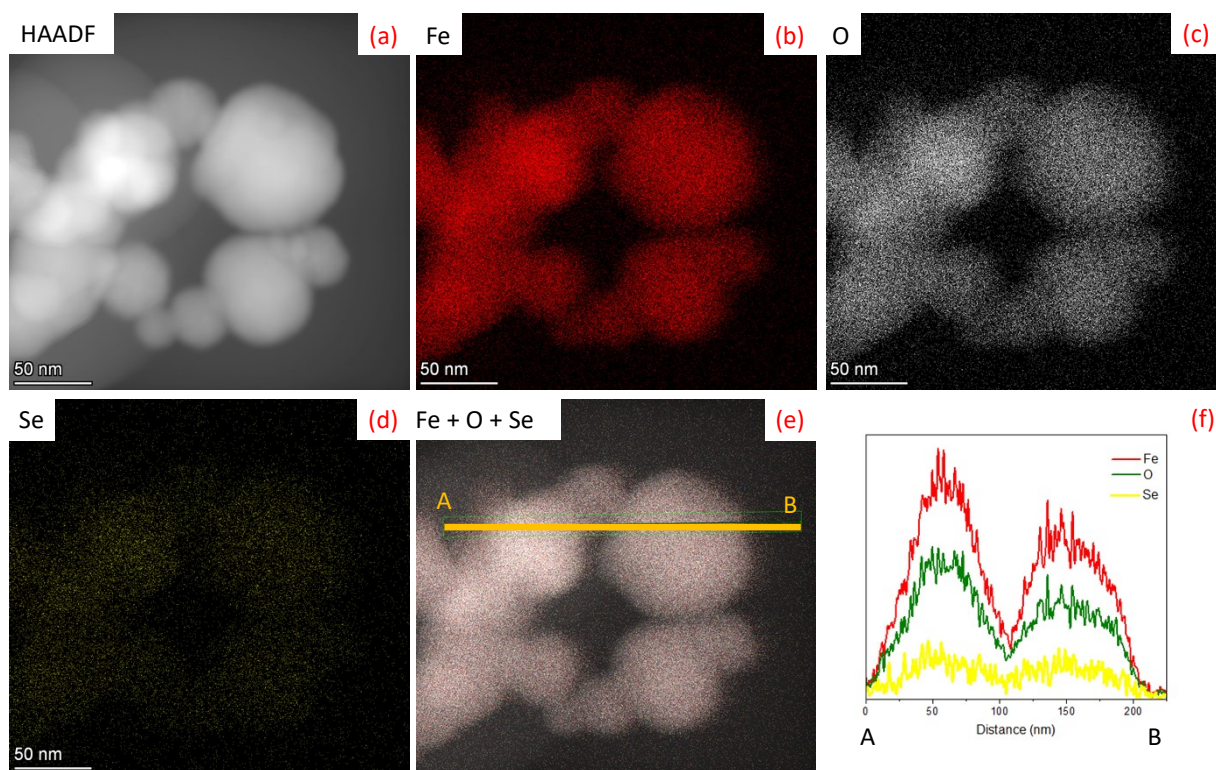


Figure S 6 STEM-EDS mapping analysis of post selenium nZVI particles; (a) HAADF image, (b) Fe mapping, (c) O mapping, (d) Se mapping, (e) Fe + O + Se mix map overlap and (f) EDS line profile for Fe, O and Se. Samples collected after 2.5 h reaction of 30 mg/L (0.38 mM) Se(VI) with 1.5 g/L nZVI.

## 10. Supporting XPS Analysis

The XPS broad survey spectra of nZVI<sub>bare</sub> and nZVI<sub>post</sub> nanoparticles are shown in Figure S 7 (a) and XPS deconvoluted Se 3d and Fe 3p spectra of nZVI<sub>post</sub> are seen in Figure S 7 (b).

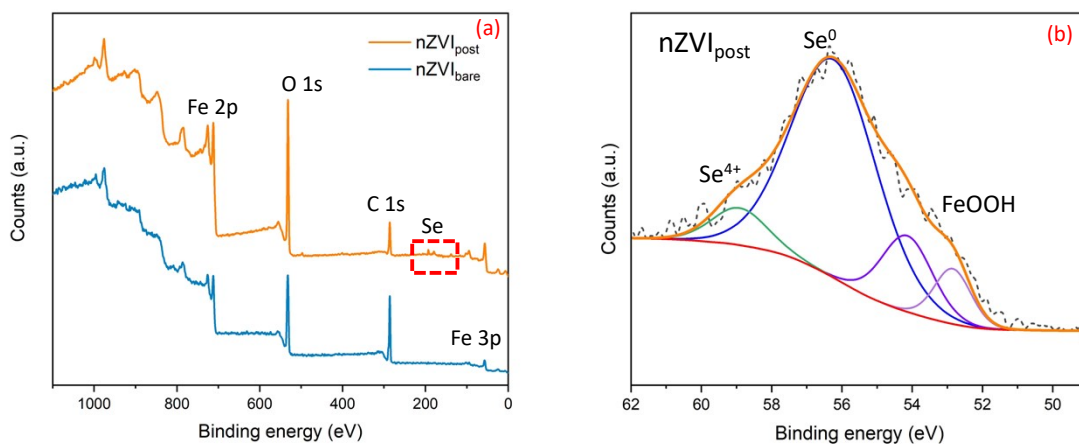


Figure S 7(a) XPS broad survey scan and (b) XPS Se 3d and Fe 3p deconvoluted spectra where binding energies overlap. *nZVI<sub>post</sub>* was analyzed after 2.5 h reaction of 30 mg/L Se(VI) with 1.5 g/L *nZVI*.

The iron (Fe 2p) and oxygen (O 1s) XPS spectra of *nZVI* before (bare) and after (post) Se deposition are shown in Figure S 8. In Table S 5 a list of the XPS peaks is given with the corresponding binding energy values [5].

Table S 5 XPS peaks and wavelengths corresponding to Figure S 8(a).

XPS peak	Binding Energy (eV)
Fe <sup>3+</sup>	728.3
Fe <sup>2+</sup>	724.7
Fe <sup>0</sup>	719.7
Fe <sup>3+</sup>	714.8
Fe <sup>2+</sup>	711.5
Fe <sup>0</sup>	706.8
Excess O or H <sub>2</sub> O	533.8
OH <sup>-</sup>	532.9
O	530.1

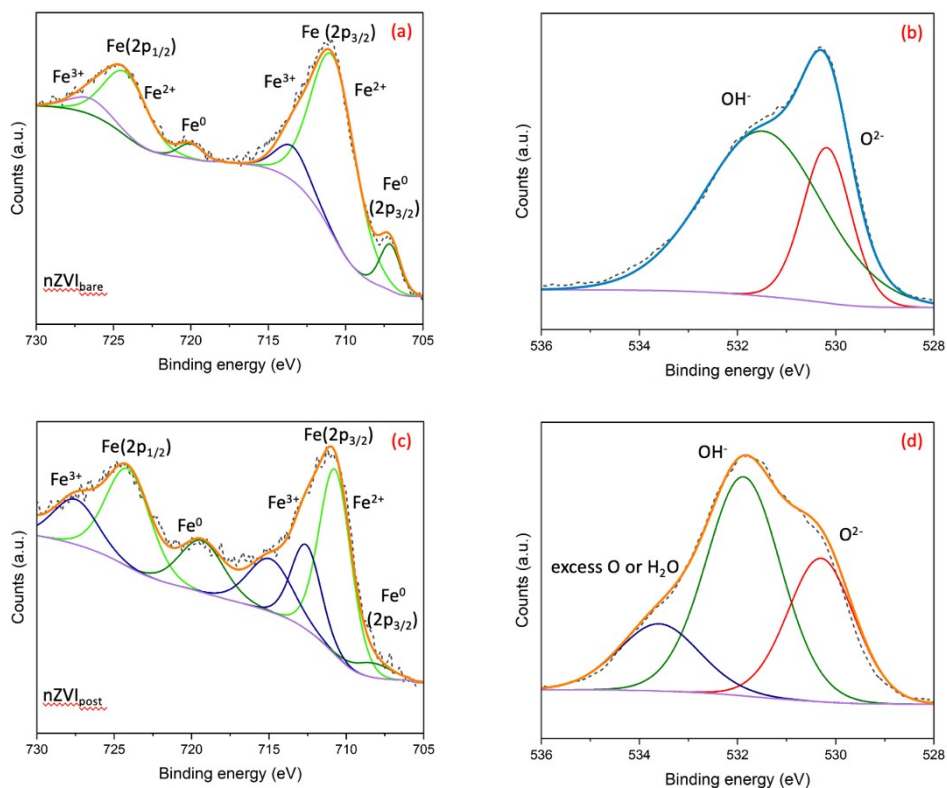


Figure S 8 XPS deconvoluted spectra of (a, c) Fe  $2p_{3/2}$  and (b, d) O  $1s$  region spectra of  $nZVI_{bare}$  and  $nZVI_{post}$  respectively. Signals were collected from  $nZVI_{post}$  after 2.5 h reactions with 30 mg/L Se(VI).

## 11. References

- [1] S. Bhattacharjee, S. Ghoshal, Optimal Design of Sulfidated Nanoscale Zerovalent Iron for Enhanced Trichloroethene Degradation, *Environmental Science & Technology* 52(19) (2018) 11078-11086.
- [2] J. Li, S. Ghoshal, Comparison of the transport of the aggregates of nanoscale zerovalent iron under vertical and horizontal flow, *Chemosphere* 144 (2016) 1398-407.
- [3] H. Liu, Q. Wang, C. Wang, X.-Z. Li, Electron efficiency of zero-valent iron for groundwater remediation and wastewater treatment, *Chemical Engineering Journal* 215 (2013) 90-95.
- [4] P. Schneider, Adsorption isotherms of microporous-mesoporous solids revisited, *Applied Catalysis A: General* 129(2) (1995) 157-165.
- [5] X.-Q. Li, W.-X. Zhang, Iron nanoparticles: The core-shell structure and unique properties for Ni (II) sequestration, *Langmuir* 22(10) (2006) 4638-4642.